Phase shift plus interpolation migration with scattering terms

Shang Huang and Daniel O. Trad

ABSTRACT

The phase shift plus interpolation (PSPI) algorithm is a useful tool to directly solve the scalar wave equation, and the results have the natural properties of the wave equation. One common issue is PSPI migration is aperture limited. In this paper, we proposed an approach that extends the illumination by adding the scattering term in PSPI migration. The benefit is keeping the input the same, which means this method does not need to estimate or modify the shot records. Iteratively adding the scattering term for each boundary layer. Numerical examples show that this improved method can recover broader illumination, for example, the horizontal events and dome structures, compared with PSPI migration only.

INTRODUCTION

Phase shift plus interpolation (PSPI) (Gazdag and Sguazzero, 1984) adapts for the media with lateral velocities variations, but it will generate discontinuity in the wavefield, which corresponds to the discontinuity in the velocity field. Based on the nonstationary filter theory (Margrave, 1998), Margrave and Ferguson (1999) came up with the nonstationary phase shift (NSPS) that can handle the velocity discontinuity with reasonable results, and have good absorbing lateral boundaries. However, the methods above have still struggled with the limited aperture for illumination.

To broaden the subsurface illumination, a scattering term that generates multiple energy (Berkhout, 2014; Davydenko and Verschuur, 2017) can be used to improve the subsurface structure prediction. In this paper, we propose a method that uses nonstationary PSPI migration with scattering term to artificially generate multiples and increase the subsurface illumination and resolution with high accuracy. Unlike the scattering term applied in full-wavefield migration, which it is generated in the forward modeling, we use that in the migration process. One benefit is that the input data keeps unchanged. There is no need to separate and correlate multiple order $i-1^{th}$ with order i^{th} during migration. Also, the computational cost will reduce with either dense or coarse shot-receiver coordination.

THEORY

In this section, phase shift plus interpolation (PSPI) migration with scattering terms algorithm will be delineated in detail along with a basic framework shown in Figure 1.

Phase shift extrapolation

From Figure 1, the first step is to extrapolate source field $D(x,z,t)$ and shot record $U(x,z,t)$ downward to the subsurface. After an initial Fourier transform over temporal space, the source and shot fields at depth z are denoted as $D(x,z,\omega)$ and $U(x,z,\omega)$ respectively.

Based on the phase shift wavefield extrapolation (Gazdag and Sguazzero, 1984) and

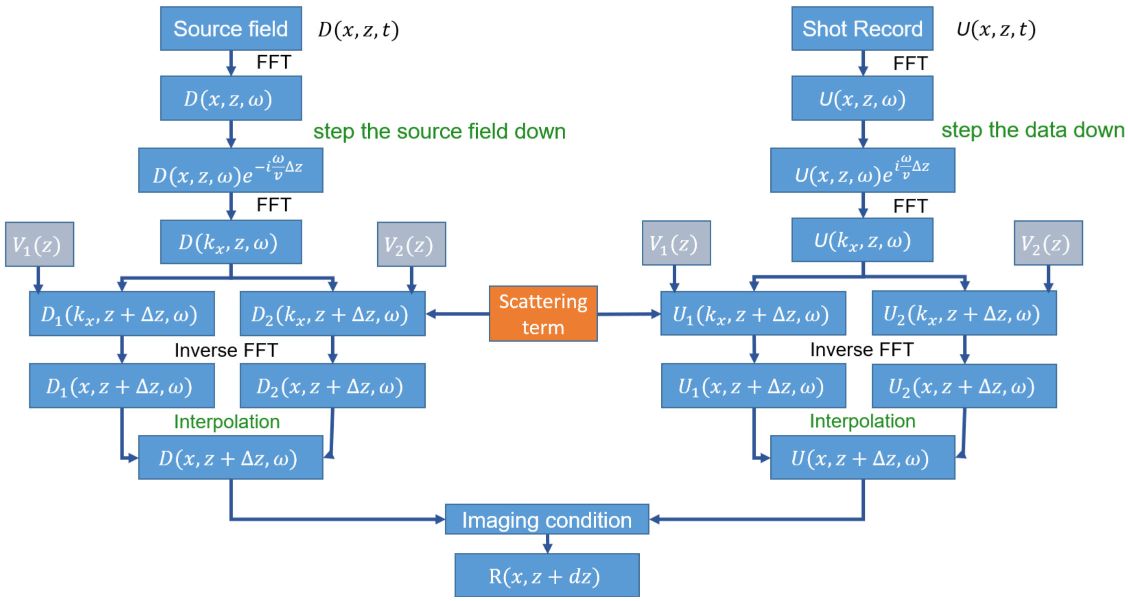

FIG. 1: Workflow for PSPI migration with scattering terms.

nonstationary phase shift (Margrave and Ferguson, 1999), the source wavefield and shot record can be stepped down by one-way wavefield extrapolation through laterally varying velocity $v(x)$:

$$D(k_x, z+\Delta z, \omega) = \frac{1}{2\pi}\int_{-\infty}^{\infty} D(x,z,\omega)\alpha_{v(x)}(k_x,x,\omega)e^{-ik_x x}\,dx, \tag{1}$$

$$U(k_x, z+\Delta z, \omega) = \frac{1}{2\pi}\int_{-\infty}^{\infty} U(x,z,\omega)\alpha_{v(x)}(k_x,x,\omega)e^{-ik_x x}\,dx, \tag{2}$$

where the shift operator $\alpha_{v(x)}(k_x,x,\omega)$ is

$$\alpha_{v(x)}(k_x,x,\omega) = \begin{cases} e^{isgn(\Delta z)k_z(x)}, & |k_x| \le \dfrac{\omega}{v(x)} \\ e^{-|\Delta z k_z(x)|}, & |k_x| > \dfrac{\omega}{v(x)} \end{cases}, k_z(x) = \sqrt{\frac{\omega^2}{v(x)^2} - k_x^2} \tag{3}$$

which ensures evanescent energy suffers exponential decay. $sgn()$ denotes the sign of depth interval for differentiating the source and shot wavefields. k_x and k_z represent horizontal and vertical wavenumber separately. Then, an ordinary inverse Fourier transform on wavenumber is applied to obtain the extrapolated wavefields in the spatial domain which will be used for wavefield interpolation with reference velocities:

$$D(x, z+\Delta z, \omega) = \int_{-\infty}^{\infty} D(k_x, z+\Delta z, \omega)e^{ik_x x}\,dk_x, \tag{4}$$

$$U(x, z+\Delta z, \omega) = \int_{-\infty}^{\infty} U(k_x, z+\Delta z, \omega)e^{ik_x x}\,dk_x. \tag{5}$$

The PSPI with scattering terms

The desired extrapolation wavefields after using reference velocities, linear interpolation (LI) and scattering term can be determined by:

$$D_{v(x)+S_D}(x, z+\Delta z, \omega) = D_{v(x)}(x, z+\Delta z, \omega) + \Delta S_D, \tag{6}$$

$$U_{v(x)+S_U}(x, z+\Delta z, \omega) = U_{v(x)}(x, z+\Delta z, \omega) + \Delta S_U, \tag{7}$$

where

$$D_{v(x)}(x, z+\Delta z, \omega) \approx \mathrm{LI}\Big(D_{v_j}(x, z+\Delta z, \omega), D_{v_{j+1}}(x, z+\Delta z, \omega)\Big), v_j \le v(x) \le v_{j+1}, \tag{8}$$

$$U_{v(x)}(x, z+\Delta z, \omega) \approx \mathrm{LI}\Big(U_{v_j}(x, z+\Delta z, \omega), U_{v_{j+1}}(x, z+\Delta z, \omega)\Big), v_j \le v(x) \le v_{j+1}, \tag{9}$$

and a small set of reference velocities are chosen for approximating the $v(x)$.

Inspired by the full wavefield migration (Davydenko and Verschuur, 2017), which uses scattering terms from the downgoing and upgoing wavefields in the frequency-space domain to predict the full-wavefield, here we have applied the scattering term but in the frequency-wavenumber domain, to simulate internal multiples. This multiple energy can help recover the subsurface illumination without sacrificing or changing the raw input data. To consider the scattering terms ΔS_D and ΔS_U effect, reference velocities from the previous depth layer is stored for computing the scattering term:

$$\Delta S_D = \int_{-\infty}^{\infty} \Big(-R(z+\Delta z)D(k_x, z+\Delta z, \omega) + R(z+\Delta z)U(k_x, z+\Delta z, \omega)\Big) e^{ik_x x}\, dk_x, \tag{10}$$

$$\Delta S_U = \Delta S_D, \tag{11}$$

where the reflectivity coefficient $R(z+\Delta z)$ is given by

$$R(z+\Delta z) = \frac{(\omega\rho(z+\Delta z))/\bar{k}_z(z+\Delta z) - (\omega\rho(z))/\bar{k}_z(z)}{(\omega\rho(z+\Delta z))/\bar{k}_z(z+\Delta z) + (\omega\rho(z))/\bar{k}_z(z)}, \tag{12}$$

where ω denotes the temporal frequency and ρ represents layer density. The vertical wavenumber $\bar{k}_z(z)$ and $\bar{k}_z(z+\Delta z)$ are determined from previous and current layer reference velocities respectively.

Imaging condition

The deconvolution imaging condition (Valenciano and Biondi, 2003) is applied in this project to obtain a stabilized reflectivity estimate:

$$I(x, z+\Delta z) = \int_{-\infty}^{\infty} \frac{D(x, z+\Delta z, \omega)^H U(x, z+\Delta z, \omega)}{D(x, z+\Delta z, \omega)^H D(x, z+\Delta z, \omega) + \epsilon}\, d\omega, \tag{13}$$

where ϵ is a stablized factor. In this way, final reflectivity estimation can be determined by summing over the temporal frequency.

In the next section, we will give some numerical examples to show that scattering terms used in the PSPI method can enlarge the subsurface illumination as well as improve the imaging result resolution.

NUMERICAL EXAMPLES

In this section, two numerical examples will be shown to demonstrate PSPI migration with scattering terms.

The first numerical example is a horizontally layered model combined with a boxcar shape anomaly in the middle depth. The model size is 511 x 251 points with 10 m spatial interval. Figure 2a and b give the true and smoothed input velocity models. Three shots with 0.8 ms time interval are located on the surface at 1800, 2800, and 3800 m separately. The number of receivers is the same as the horizontal points. A fourth-order finite difference method is used for forward modeling which is shown in Figure 2c.

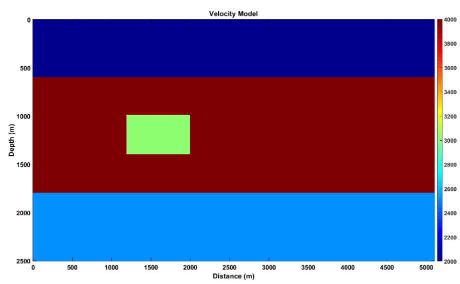

(a)

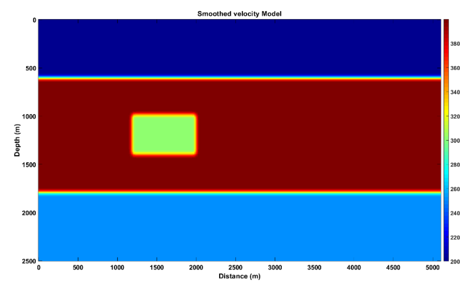

(b)

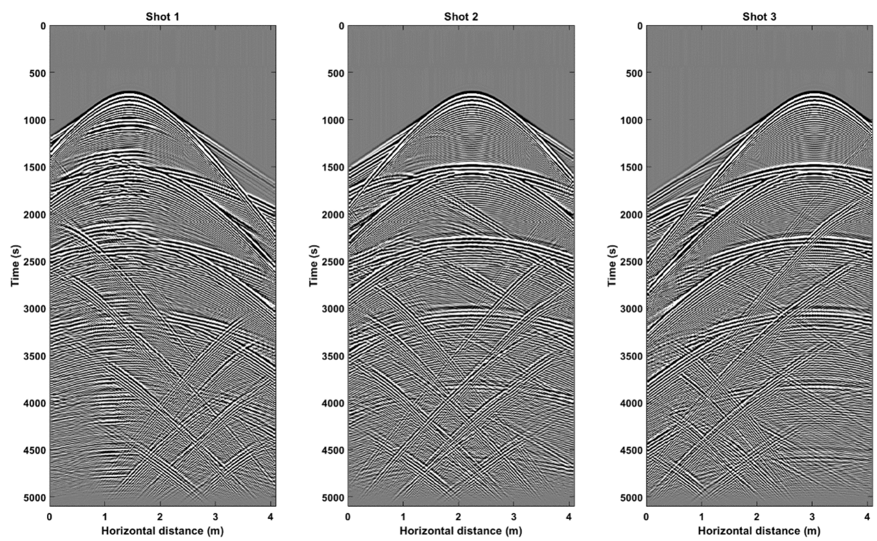

(c)

FIG. 2: (a) True velocity model. (b) Smoothed velocity model. (c) Shot records simulated at 1800, 2800, and 3800 m on the surface.

Figure 3a gives PSPI migration result without scattering term. The first reflector at 500 meters depth has been recovered with high amplitudes, but the boxcar anomaly as well as the deep horizontal event cannot be predicted accurately. Also, both shallow and deep parts have artifacts by wavefield interference. On the other hand, Figure 3b which uses scattering term can give an accurate migrated location for the subsurface structure. For example, the boxcar anomaly prediction between depth 1000 and 1500 meters has larger amplitudes on the side boundaries compared with Figure 3a. The deep horizontal layer at around 1800 meters can be reconstructed with higher resolution by adding scattering term than not using it. Furthermore, the shallow part artifacts is suppressed after adding scattering term in the migration process.

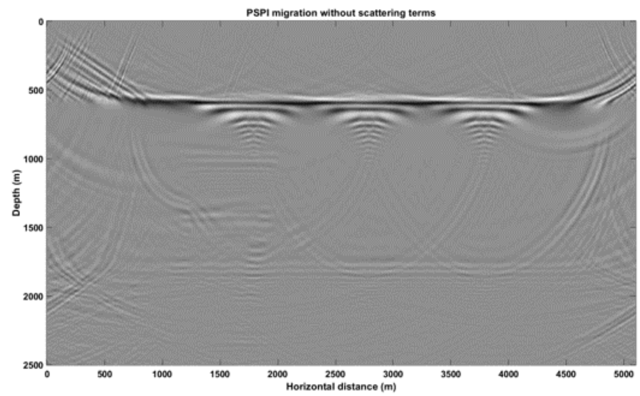

(a)

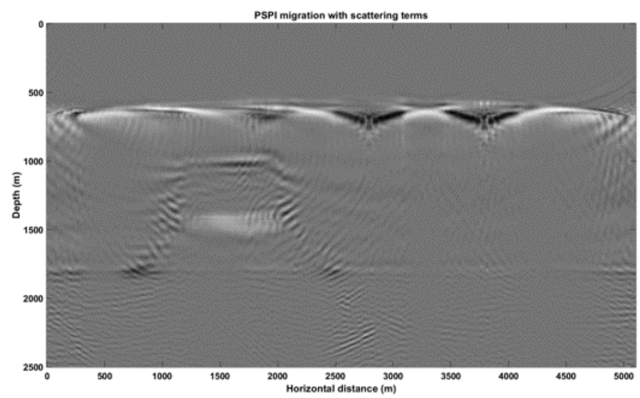

(b)

FIG. 3: (a) PSPI migration without scattering term; (b) PSPI migration with scattering terms.

The second numerical example turns to a more complicated case where adding a curvature shape anomaly. The settings including horizontal distance, depth, time and space intervals, number of shots and receivers are the same as the previous example. Figure 4a and b show the true and smoothed velocity models and Figure 4c demonstrates the shot records obtained from a horizontal distance at 500, 1000 and 1500 meters separately.

For the boxcar shape structure, the results show a similar result as the previous example. The scattering terms (Figure 5)b help PSPI migration to locate where the anomaly is since it provides the side boundary information. As for the curvature-boxcar combined anomaly, Figure 5a cannot recover the details of the structure shape, only gives rough information for the left side boundary like between 2500 m and 3500 m in the horizontal distance; however, Figure 5, using scattering term in migration, can migrate correct anomaly's top boundary as well as the dome structure. Nevertheless, it cannot specify the thin layers due to the coarse shot coordination, like between the dome bottom boundary and horizontal

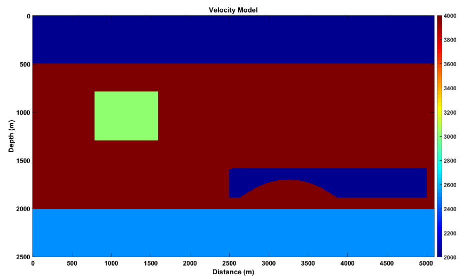

(a)

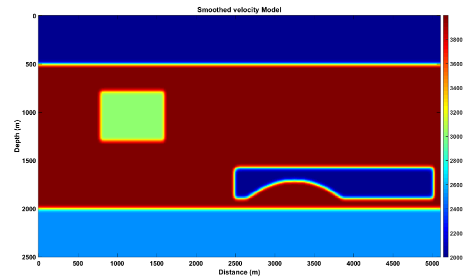

(b)

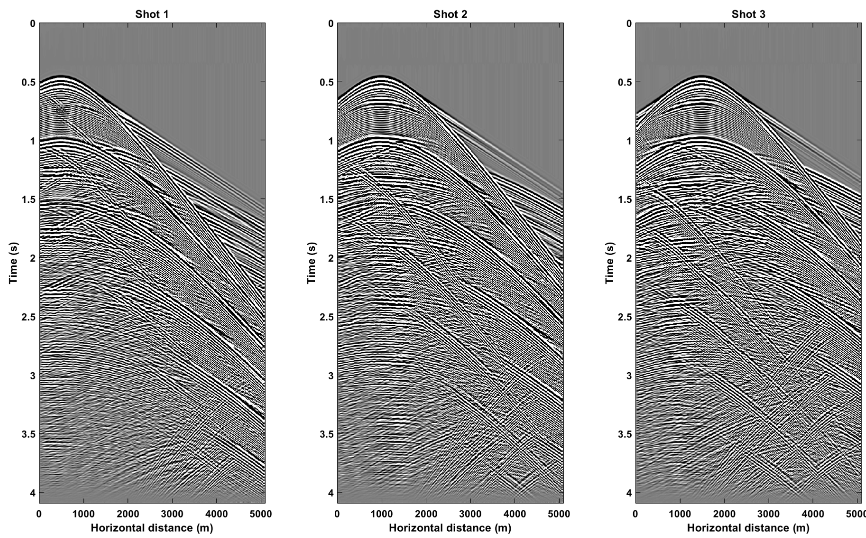

(c)

FIG. 4: (a) True horizontal-layered velocity model. (b) Smoothed horizontal-layered velocity model. (c) Shot records.

layer. For the deep horizontal event, PSPI migration with the scattering term can predict a higher resolution reflector than Figure 5a, but with more artifacts below the event. The next step for this research is to try to remove the incoherent noise in the result.

CONCLUSIONS

When given the coarse shot coordination, PSPI migration with scattering terms can recover broader reflectors with higher resolution and amplitudes compared with the situation that without scattering terms. Furthermore, our proposed method can suppress artifacts on the shallow depth generated by wavefield interference. However, even though PSPI migration with scattering term migrates the accurate reflector location at the deeper structure, the noise also shows up which needs to be removed in future work.

ACKNOWLEDGEMENTS

The authors would like to thank the sponsors of CREWES for continued support. This work was funded by CREWES industrial sponsors, China Scholarship Council (CSC) and NSERC (Natural Science and Engineering Research Council of Canada) through the grants

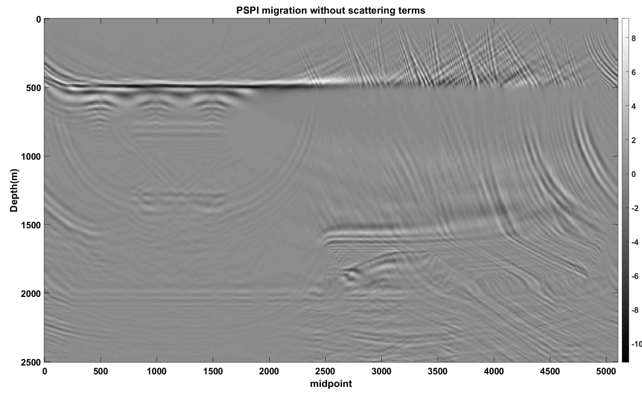

(a)

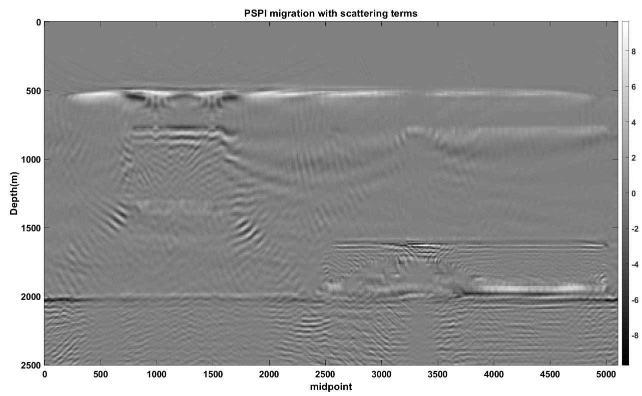

(b)

FIG. 5: (a) PSPI migration without scattering term; (b) PSPI migration with scattering terms.

CRDPJ 543578-19.

REFERENCES

Berkhout, A., 2014, An outlook on the future of seismic imaging, part ii: Full-wavefield migration: Geophysical Prospecting, **62**, No. 5, 931–949.

Davydenko, M., and Verschuur, D., 2017, Full-wavefield migration: using surface and internal multiples in imaging: Geophysical Prospecting, **65**, No. 1, 7–21.

Gazdag, J., and Sguazzero, P., 1984, Migration of seismic data by phase shift plus interpolation: Geophysics, **49**, No. 2, 124–131.

Margrave, G. F., 1998, Theory of nonstationary linear filtering in the fourier domain with application to time-variant filtering: Geophysics, **63**, No. 1, 244–259.

Margrave, G. F., and Ferguson, R. J., 1999, Wavefield extrapolation by nonstationary phase shift: Geophysics, **64**, No. 4, 1067–1078.

Valenciano, A. A., and Biondi, B., 2003, 2-d deconvolution imaging condition for shot-profile migration, *in* SEG Technical Program Expanded Abstracts 2003, Society of Exploration Geophysicists, 1059–1062.